ACS APPLIED ENERGY MATERIALS

www.acsaem.org Article

Are Polyaniline and Polypyrrole Electrocatalysts for Oxygen (O_2) Reduction to Hydrogen Peroxide (H_2O_2)?

Hannah Rabl, Dominik Wielend,* Serpil Tekoglu, Hathaichanok Seelajaroen, Helmut Neugebauer, Nikolas Heitzmann, Dogukan Hazar Apaydin, Markus Clark Scharber, and Niyazi Serdar Sariciftci

Cite This: *ACS Appl. Energy Mater.* 2020, 3, 10611−10618 Read Online

ACCESS | Metrics & More | Article Recommendations | Supporting Information

ABSTRACT: In this report, we present results on the electrocatalytic activity of conducting polymers [polyaniline (PANI) and polypyrrole (PPy)] toward the electrochemical oxygen reduction reaction (ORR) to hydrogen peroxide (H_2O_2). The electropolymerization of the polymers and electrolysis conditions were optimized for H_2O_2 production. On flat glassy carbon (GC) electrodes, the faradaic efficiency (FE) for H_2O_2 production was significantly improved by the polymers. Rotating disc electrode (RDE) studies revealed that this is mainly a result of blocking further H_2O_2 to the water reduction pathway by the polymers. PPy on carbon paper (CP) significantly increased the molar production of H_2O_2 by over 250% at an average FE of above 95% compared to bare CP with a FE of 25%. Thus, the polymers are acting as catalysts on the electrode for the ORR, although their catalytic mechanisms differ from other electrocatalysts.

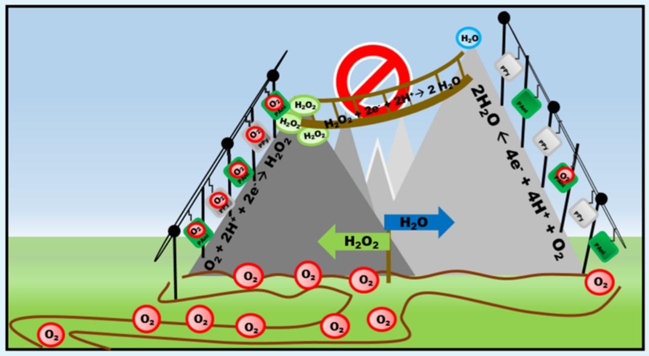

KEYWORDS: *electrocatalysis, oxygen reduction, conducting polymers, polyaniline, polypyrrole, hydrogen peroxide production*

1. INTRODUCTION

In order to reduce the dependence on fossil fuels, great effort is made on exploration and utilization of inexhaustible and renewable energy sources such as solar energy.[1,2] To overcome the bottleneck of coordination in between energy supply and demand, we need long-term energy storage systems. As such, commercial batteries nowadays still do not possess the required energy and power density as global storage media. On the other hand, energy-carrying chemicals (synthetic fuels) formed through the electrocatalytic conversion of water (H_2O) and carbon dioxide (CO_2) are an interesting route because for storage and transportation of the products, the existing industrial energy infrastructure can be used. Alternatively, oxygen (O_2) reduction products such as hydrogen peroxide (H_2O_2) have been investigated as high energy density carriers.[3−5] Besides a potential use as a fuel, H_2O_2 is a versatile chemical with high demand for several applications such as organic synthesis,[6−8] paper production,[8,9] sanitizing, and bleaching.[8]

According to its unique feature of being an oxidizing agent as well as a reducing agent, it was introduced to the instrumentation of smart and delocalized fuel cells in a one-compartment cell configuration.[10−12] Independent of the energy release pathway, the reaction products are either O_2 or H_2O, of which both are, for example, educts for hydrogen peroxide production, offering a complete chemical recycling.

Today, H_2O_2 is mostly produced through the hydrogenation of soluble anthraquinone derivatives followed by oxidation—the so-called anthraquinone-oxidation process.[6,8] As this process demands high energy input for product separation, environmentally friendly alternatives are sought. One of the promising approaches is the electrochemical reduction of oxygen,[13,14] which interestingly has been investigated since early 1900s. Although the earliest report for electrochemical H_2O_2 synthesis was in 1901 by Meidinger[15] using platinum electrodes, in 1939, Berl[16] was the first one reporting the activity of carbon-based electrodes toward H_2O_2 production. The focus of this present work is on electrocatalysis using carbon-based and organic electrocatalysts, where various materials such as glassy carbon (GC), carbon nanotubes (CNTs),[13] and nitrogen-doped mesoporous carbon materials[17] have already been reported to show high efficiencies toward H_2O_2 production. Moreover, organic pigments[18] such as quinacridone, epindolidione,[19] and perylenediimide[20] have been reported for their capability of being (photo-)-electrocatalysts for the production of H_2O_2. Besides inves-

Received: July 14, 2020
Accepted: September 29, 2020
Published: September 29, 2020

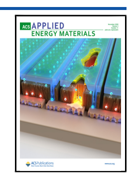

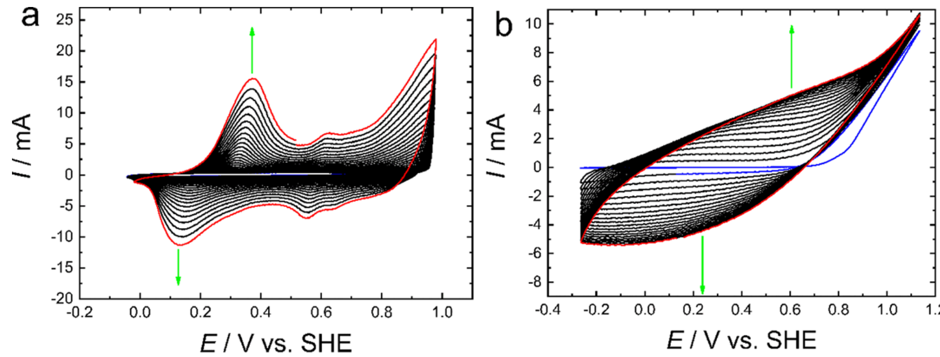

Figure 1. (a) Potentiodynamic polymerization of 0.1 M aniline in 0.5 M H_2SO_4 electrolyte solution for 25 cycles at a scan rate of 25 mV s^{-1}, (b) potentiodynamic polymerization of 0.45 M pyrrole in 0.15 M PBS solution for 20 cycles at a scan rate of 50 mV s^{-1}. The first cycle is shown in blue color, and the last cycle is shown in red color.

tigation of new organic catalysts in general to achieve the industrial demand of stable electrocatalysts, additional research on electrode surface engineering[21] or immobilization of known electrocatalytic compounds such as anthraquinone on CNT's[22] is also reported.

One promising class for organic electrocatalysts are the well-studied "organic metallic polymers, that are, conducting polymers",[23−26] organic compounds which become conductive upon doping, such as polyanilines (PANI), polypyrroles (PPy), or polythiophenes. Throughout the last decades, numerous reports have been published for energy storage applications,[27−30] batteries,[31−33] supercapacitors,[34] sensors,[35] solar cells, or transistors.[36]

In the 1980s, Mengoli *et al.*[37,38] as well as Cui and Lee[39] reported the electrochemical reduction of oxygen on PANI electrodes. Later, Khomenko *et al.*[40] described the electrocatalytic properties for PANI and PPy toward oxygen reduction, but disproved such a behavior for poly(3,4-ethylenedioxythiophene) (PEDOT). Regarding PEDOT, controversial reports exist in the literature; moreover, PEDOT has been proposed as selective H_2O_2 to water electrocatalyst,[41] but in a consecutive work, the same group reported a selective O_2 to H_2O_2 reduction catalyzed by PEDOT.[42] As the reduction step of H_2O_2 to H_2O depends strongly on the existing overall H_2O_2 concentration, this may be origin of these controversial reports. Ramiréz-Pérez *et al.* chemically synthesized and pyrolyzed carbon fiber/PPy composites for the oxygen reduction reaction (ORR).[43] Many recent studies[44−46] explore the electrocatalytic effect of pyrolyzed compounds also derived from conducting polymers, but direct comparison to the unmodified polymers is difficult.

It has to be noted that because of the synthetic parameters chosen for the polymerization, those conductive polymers might be doped with metal ions which are known to catalyze oxygen reduction, where the intended doping with metals is sometimes even the goal by the preparation and investigation of polyaniline-metal particle[47,48] composites for the ORR.[49] In recent years, the group of Azzaroni investigated numerous promising approaches of gaining synergistic effects of the combination of PANI with metal−organic frameworks for an enhanced ORR.[50−52] PANI and PEDOT were also used as the polymer matrix for incorporated metal particles for the ORR as well as the electrochemical hydrogen evolution reaction (HER),[53,54] and recently, even pure PANI was described as an electrocatalyst itself for the HER.[55]

The motivation for the present work has been the investigation of electropolymerized PANI and PPy films on GC and carbon paper (CP) electrodes, which are free of metal dopants. These two different carbon electrodes were chosen as models of flat and high-surface electrodes, respectively. The electrocatalytic activity of PANI and PPy toward oxygen reduction to H_2O_2 was investigated by combining the techniques of cyclic voltammetry (CV), chronoamperometry, and rotating disc electrode (RDE) characterization.

2. EXPERIMENTAL SECTION

2.1. Electrode Preparation. 2 mm thick GC (Alfa Aesar, Type1) electrodes were polished prior to use for 1 min each with Buehler Micropolish II deagglomerated alumina in decreasing particle size from 1.0 to 0.3 to 0.05 μm. In between, the electrodes were sonicated for 15 min each in 18 MΩ water (MQ water) and isopropanol (VWR Chemicals).

Electrochemical treatment of GC was performed by sweeping the potential in a 0.5 M H_2SO_4 solution between +1500 and −1000 mV vs Ag/AgCl (3 M KCl) at a scan rate of 50 mV s^{-1} for 30 cycles.

To prepare Cr-/Au-coated glass electrodes for spectroscopy, glass slides were cut into the size of 0.7 × 6.0 cm and subsequently cleaned *via* sonication in the following solvents for 15 min each: acetone (VWR Chemicals), 2% Hellmanex solution (Hellma-Analytics), MQ water, and isopropanol. Afterward, the samples were treated for 5 min at 50 W in the oxygen plasma oven Plasma ETCH P25. In a thermal metal evaporation chamber, 5 nm chromium followed by 80 nm of gold was deposited at ~10^{-6} mbar.

Toray CP (Alfa Aesar, TGP-H 60) was used as received and cut into an appropriate size of 1.0 × 3.0 cm.

2.2. Electrochemical Polymerization. Following the reported procedures of Nunziante and Pistoia,[56] as well as Sariciftci *et al.*[57] after optimization (see Supporting Information, Figures S1−S4), the potentiodynamic oxidative electropolymerization of aniline was performed in 0.5 M H_2SO_4 (J.T.Baker) in a one-compartment cell. The cell was purged with nitrogen (N_2) for 45 min before aniline (Sigma-Aldrich, freshly distilled) was added to obtain a concentration of 0.1 M. After additional 15 min of N_2 purging, the electrodes [Pt as the counter electrode (CE) and the saturated calomel electrode (SCE) as the reference electrode (RE)] were equipped and the polymerization was performed by sweeping between +800 and −200 mV at a scan rate of 25 mV s^{-1} for 25 cycles (see Figure 1a).

Developed from the procedure for chemical synthesis in phosphate-buffered saline (PBS) solution [containing 0.137 M NaCl (ACM), 2.7 mM KCl (Alfa Aesar), 0.01 M Na_2HPO_4 (Sigma-Aldrich), and 1.8 mM KH_2PO_4 (Sigma-Aldrich)] by Andriukonis *et al.*,[58] potentiodynamic oxidative electropolymerization of pyrrole (see Figure 1b) was performed, to which pyrrole was added resulting in a concentration of 0.45 M. The emulsion was stirred vigorously. Pt was used as the CE, and Ag/AgCl(3 M KCl) as the RE. The

https://dx.doi.org/10.1021/acsaem.0c01663
ACS Appl. Energy Mater. 2020, 3, 10611−10618

electropolymerization was performed without stirring by sweeping the potential between −400 and 1000 mV at a scan rate of 50 mV s^{-1} for 20 cycles.

2.3. Electrochemical Experiments. Electrochemical characterization of obtained polymers (CV and chronoamperometry) was done using a Jaissle Potentiostat-Galvanostat 1030 PC-T and a Jaissle Potentiostat-Galvanostat PGU10V-100 mA. The experiments were performed in a two-compartment cell (separated with a glass frit) using 20.0 mL of electrolyte solution. Regarding the current density (j) in all cases, the geometric electrode area was taken into consideration.

The electrolyte solutions of 0.5 M H_2SO_4 (J. T. Baker), 0.1 M $NaHSO_4$ (Alfa Aesar), and 0.1 M NaOH (Merck) were prepared by dissolving the corresponding amount in MQ water. The 0.1 M phosphate buffer (PB) solution was prepared from K_2HPO_4 (Sigma-Aldrich) and KH_2PO_4 (Sigma-Aldrich), resulting in a pH of 7.

Prior to the electrochemical measurements, the cell was purged with N_2 for 1 h in order to achieve nitrogen-saturated conditions. Then, 30 min purging with O_2 gas was done to provide oxygen-saturated conditions. Unless stated elsewise, a platinum plate was used as the CE, a commercial Ag/AgCl (3 M KCl) (BASi) as the RE, and a scan rate of 20 mV s^{-1} was applied in all CV experiments.

Chronoamperometric electrolysis experiments were performed for 6 h at a constant potential, which was recalculated to the potential of the standard hydrogen electrode (SHE). During the experiment, 100 μL aliquots of the electrolyte solution were taken several times and used for H_2O_2 quantification. In order to prove the reproducibility of the experiments, repetitions under identical conditions were used for statistical calculation of mean values, and accordingly, error bars for at least three individual sets of experiments are shown. For the reduction processes for O_2, the two products H_2O_2 and H_2O are possible, as illustrated in Scheme 1.

Scheme 1. Schematic Illustration of the 2- and 4-Electron Reduction Pathways for the Oxygen Reduction

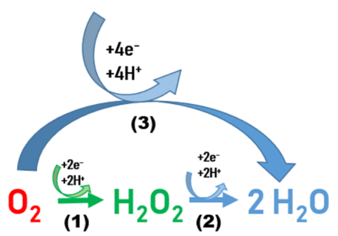

The Faradaic Efficiency for H_2O_2 was calculated by

$$\% \text{ FE} = \frac{n_{\text{product}}}{\frac{1}{n_{\text{reaction}}} \cdot \text{moles of electrons}} * 100 \quad (1)$$

using $n = 2$ as H_2O_2 is the product of the two-electron reduction of O_2.

Hydrodynamic electrochemical characterization with RDE measurements was performed on an IPS Jaissle PGU BI-1000 Bipotentiostat-Galvanostat attached to an IPS PI-ControllerTouch unit and an IPS Rotator 2016 rotating unit. A GC disc (Ø = 8 mm) in polychlorotrifluoroethylene (PCTFE)was used as WE and polished in the same manner similar to the GC plate mentioned above. An Ag/AgCl (3 M KCl) (Messtechnik Meinsberg) electrode in a Luggin capillary was used as the RE and a platinized electrode as the CE. Rotating ring-disc electrode (RRDE) measurements were performed using a GC disc (Ø = 5 mm) in polyether ether ketone (PEEK) with a Pt ring (Ø = 7 mm). In all linear sweep voltammetry (LSV) measurements under convection, a sweep rate of 10 mV s^{-1} was applied.

Unless stated elsewhere, all potentials mentioned in this work are recalculated and refer to the SHE.

2.4. Characterization Methods. Spectroscopic characterization of the obtained polymer-coated electrodes was done using attenuated total reflection Fourier transform infrared spectroscopy (ATR-FTIR) and Raman spectroscopy. ATR-FTIR was performed on a Bruker VERTEX 80-ATR spectrometer in the spectral range of 3600−500 cm^{-1}. Raman spectroscopy was performed on a Bruker MultiRAM Raman Microscope using an excitation wavelength of 1064 nm in the spectral shift range between 3600 and 5 cm^{-1} (see Figures S6 and S7).

The morphology of the prepared electrodes was analyzed by scanning electron microscopy (SEM). A JEOL JSM-6360LV scanning electron microscope was operated under high vacuum settings, and an acceleration voltage of 7.0 kV and a SEM ZEISS 1540 XB cross-beam scanning electron microscope operated at 3.0 kV was used.

The quantification of produced H_2O_2 was done according to the previously reported colorimetric method.[59,60] (see Supporting Information, Figure S5 for further details).

3. RESULTS AND DISCUSSION

The first step was to prepare and investigate polyaniline and polypyrrole coated on GC electrodes (GC/PPy). Raman and ATR-FTIR spectra of the obtained PANI and PPy films are presented in Supporting Information, Figures S6 and S7, while the CV curves of optimized electropolymerizations of PANI and PPy are shown in Figure 1.

The polymerization CV curves in Figure 1 show a gradual increase in current over performed cycles with the reversible oxidation of PANI from the fully reduced leucoemeraldine form to the half-oxidized emeraldine form at potentials 0−250 mV and further to the fully oxidized pernigraniline form in the potential range of 600−800 mV and subsequent re-reduction to the nonconducting, leucoemeraldine form.[61]

In Figure 2, the SEM images of electropolymerized PANI and PPy on GC as well as CP are shown.

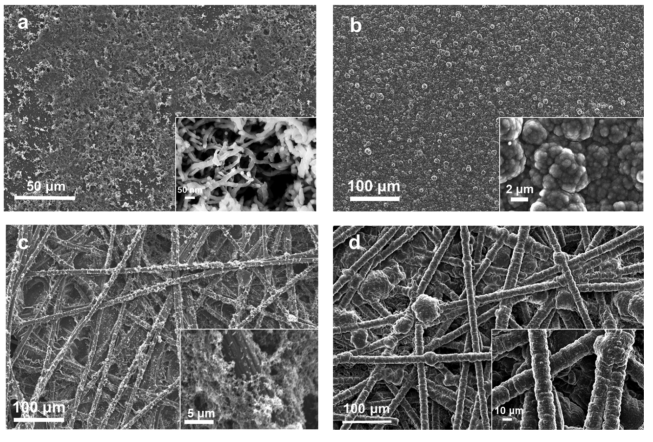

Figure 2. (a) SEM images of PANI polymerized on a GC electrode. (b) SEM images of PPy polymerized on a GC electrode. (c) SEM images of PANI polymerized on a CP electrode. (d) SEM images of PPy polymerized on a CP electrode.

The SEM images in Figure 2a show that PANI in a sponge-like structure covered a major fraction of the GC surface. The inset reveals that the structure was composed of individual cross-linked fibers. In contrast, the SEM images of a PPy electrode in Figure 2b,d show a full coverage of globule-like polypyrrole structures on all visible carbon structures. For further comparison, SEM images of bare CP are shown in Supporting Information, Figure S8.

Figure 3a shows that a GC/PANI as well as a bare GC (see Figure S9) show almost flat CV curves under the N_2 atmosphere and a distinct reductive peak at −200 mV under

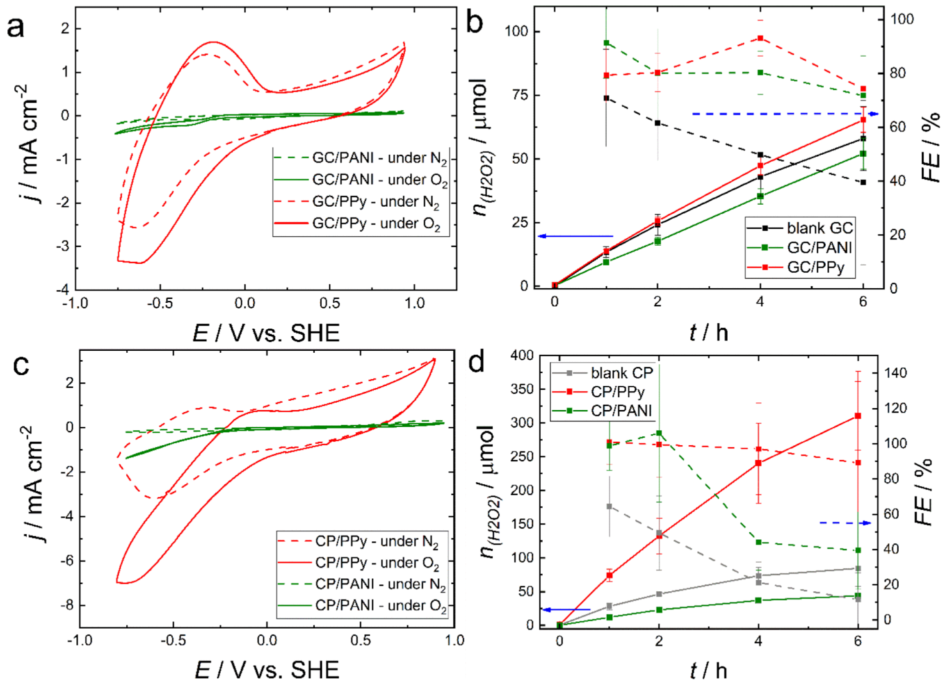

Figure 3. (a) CV of GC/PANI and GC/PPy in 0.1 M PB (at pH 7) w/o O_2. (b) Results of chronoamperometry of blank GC as well as GC/PANI and GC/PPy in 0.1 M PB at −400 mV vs SHE including the faradaic efficiency (FE) for H_2O_2 (c) CV of CP/PANI and CP/PPy in 0.1 M PB (at pH 7) w/o O_2. (d) Results of chronoamperometry of blank CP as well as CP/PANI and CP/PPy in 0.1 M PB at −400 mV vs SHE including the FE for H_2O_2. In the graphs b and d, continuous lines describe moles H_2O_2 and dashed lines are used for presenting FE values.

O_2 reflecting the ORR. Besides the CV result in Figure 3a, by performing chronoamperometry at various pH solutions and at different applied potentials, chronoamperometry at −400 mV vs the SHE showed the highest H_2O_2 production yield (see Supporting Information, Figure S10). Because of these findings, further chronoamperometry was performed at this potential for 6 h and the results are shown in Figure 3b. As the moles of H_2O_2 remained quite unchanged because of the current observed in the transient curves in the case of GC/PANI (Figure S11), the faradaic efficiencies toward H_2O_2 production were improved from roughly 40% in the bare GC case to 80% in a GC/PANI case. This is because of the lower conductivity of the PANI layer under these conditions, which caused a higher serial resistance. A similar result was observed while operating in an acidic solution (pH 2) (Figure S12). Moreover, different PANI redox features and slightly lower H_2O_2 quantities were found. One possible explanation for this enhancement of the FE might be that PANI acts somehow as a layer directing to the H_2O_2 reaction pathways. Electrocatalytic investigations on electrode materials favoring the direct 4-electron reduction of O_2 to H_2O similar to platinum did not show any improvement through a PANI layer. To further investigate this possibility of PANI as a peroxide directing layer, the same set of experiments was performed using a high-surface area carbon electrode, CP (Figure 3c,d).

In order to examine another conductive polymer besides PANI, PPy was also investigated using both GC and CP electrodes. The CV curves in Figure 3c show that using CP, significantly larger current densities of the redox-active polypyrrole were obtained because of the larger electroactive surface area of CP as compared to GC. In addition, upon O_2-saturated conditions, CP/PPy showed a pronounced reductive current of nearly 7 mA cm^{-2} at −700 mV as compared to about 3 mA cm^{-2} observed under N_2-saturated conditions (see Figure S9). During chronoamperometry experiments, the amount of produced H_2O_2 and the corresponding FE toward the electrocatalytic oxygen reduction to H_2O_2 are shown in Figure 3d. Comparing bare CP to GC, it showed higher H_2O_2 production but a substantially lower FE. The CP/PPy electrode significantly enhanced the H_2O_2 production up to 300 μmoles after 6 h at a FE close to 100%. This result is in good agreement to a previous work by Wu, Venancio, and MacDiarmid,[33] and Raminéz-Pérez *et al.*[43] which underline the electrocatalytic properties of PPy, especially of the "nanomaterial PPy" they investigated. Although Wu *et al.*[33] and Khomenko *et al.*[40] reported an electrocatalytic behavior accompanied with a current increase, we could just observe increased FE for H_2O_2 with our electrochemically polymerized PANI.

In comparison to bare GC, GC/PPy (Figure 3b) showed an enhancement of the H_2O_2 produced at a comparable high FE of nearly 80%. The electrocatalytic properties of PPy toward H_2O_2 production under acidic conditions at pH 2 were also investigated (Figure S14). A slightly increased H_2O_2 production was observed, but the determined FE was either similar or even lower than a blank CP.

These observations reveal the evidence that PPy on CP considerably enhances the H_2O_2 production quantities with improved FE. In order to gain further insights into the mechanistic details of the reactions on bare GC as well as on polymer-coated GC, hydrodynamic-voltammetric experiments were performed. The obtained faradaic efficiencies of GC for H_2O_2 production, which were determined by RRDE, are shown in Figure 4.

As illustrated in Scheme 1, in general, oxygen can be reduced *via* a four-electron reduction process directly to water (pathway 3) or *via* a two-electron reduction process to H_2O_2 (pathway 1). Hydrogen peroxide can also be further reduced

https://dx.doi.org/10.1021/acsaem.0c01663
ACS Appl. Energy Mater. 2020, 3, 10611−10618

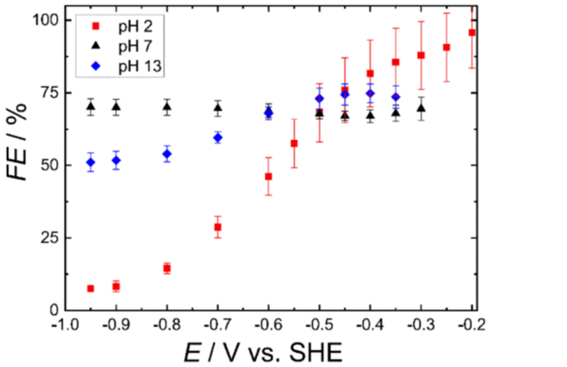

Figure 4. Faradaic efficiencies for H_2O_2 production determined on GC *via* RRDE in 0.1 M $NaHSO_4$ (pH 2), 0.1 M PB (pH 7), and 0.1 M NaOH (pH 13).

to water by a subsequent two-electron reduction process (pathway 2). As H_2O_2 is an electroactive species which can be determined on a platinum ring, the FE of H_2O_2 produced at the GC disc can be calculated from the disc current (I_D) and the ring current (I_R) at a certain applied potential, respectively (See Supporting Information, Figures S15 and S16 for further details). At moderate cathodic potentials at pH 2, a high selectivity toward H_2O_2 production was observed, which gradually decreased to nearly zero at potentials that were more negative than −0.8 V. At neutral pH, the efficiency was constant over the whole investigated potential range, while under alkaline conditions, a maximum FE of 75% was observed at −0.5 V. All of the results obtained by this RRDE method are in good agreement with the literature reports[62,63] as well as to the FE values determined by the abovementioned chronoamperometry at −0.4 V after 1 h electrolysis.

To compare these results from blank GC with polymer-coated electrodes, RDE investigations of GC/PANI were performed as shown in Figure 5.

The LSV curves of GC/PANI at pH 7 in Figure 5a look similar to one of the blank GC and upon the addition of H_2O_2, a slightly increased *j* was observed. Deriving the number of transferred electrons (*n*) by Koutecki−Levich-Analysis (K−L) GC/PANI as well as GC show a pronounced tendency for the two-electron H_2O_2 production pathway at potentials between −0.3 and −0.6 V. At more negative potentials under the O_2 atmosphere, no significant onset for further reduction to H_2O was observed. Upon H_2O_2 addition, GC showed a steep increase in *n*, reflecting more H_2O_2 reduction reaction. This behavior was also observed for GC/PANI but with a moderately increased *n* at potentials lower than −0.6 V. Analysis of blank GC and GC/PANI at pH 2 (Figure S17) revealed that at potentials lower than −0.5 V, a similar behavior at neutral pH was observed, followed by a further reduction of oxygen to water at more negative potentials of around −1.0 V. In accordance with the results at pH 7, the addition of H_2O_2 led to an increased cathodic current, although in general *j* was significantly lower in the acidic medium compared to the neutral one. As a consequence of the very low *j* values, K−L analysis could only be performed at the potentials which were more negative than −0.7 V. Concluding from Figure 5d, GC/PANI at pH 2 acted as a *peroxide-directing layer* which shifted the onset potential for H_2O_2 reductions to more negative potentials. Comparing to chronoamperometry experiments (Figure S12), these results showed a similar produced H_2O_2 amount but a higher FE, which was obviously a result of the hindrance of undesired H_2O_2 reduction and a lower current as a result of a higher serial resistance. Although recent reports[55] somehow proposed that PANI in the acidic

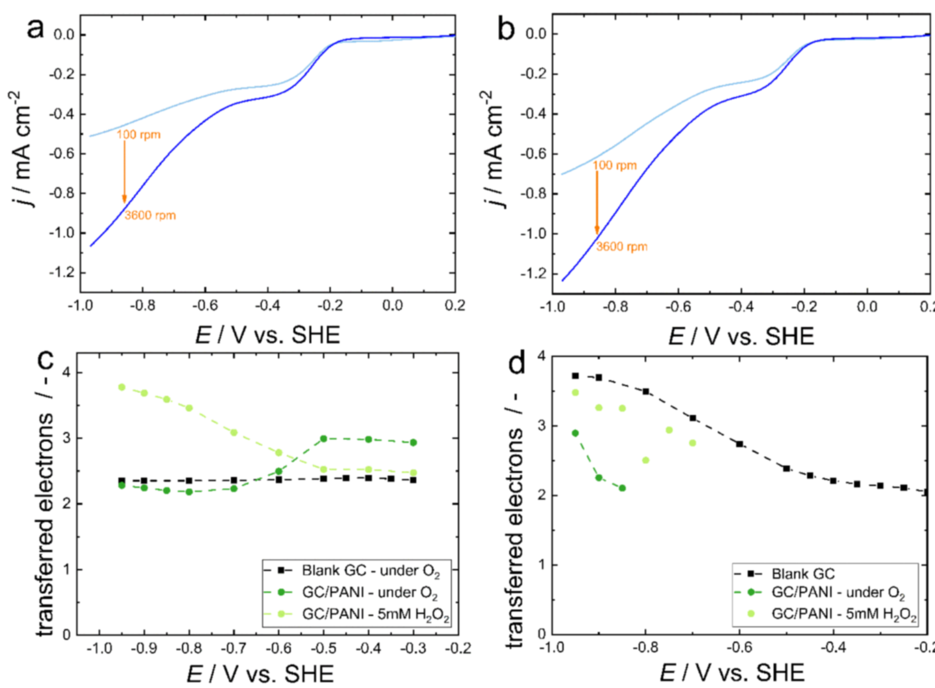

Figure 5. (a) LSV of GC/PANI at pH 7 under O_2 and (b) LSV of GC/PANI at pH 7 under O_2 with H_2O_2 added (c) number of electrons transferred of GC as well as GC/PANI at pH 7 [calculated from results in (a) and (b)] (d) number of electrons transferred of GC as well as GC/PANI at pH 2 (calculated from results in Figure S16b,c).

https://dx.doi.org/10.1021/acsaem.0c01663
ACS Appl. Energy Mater. 2020, 3, 10611−10618

medium acted as an electrocatalyst for hydrogen evolution, our results cannot confirm these findings for pH 2.

In addition to the RDE investigations of GC/PANI, GC/PPy was tested in both neutral and acidic media toward the ORR. In analogy to GC/PANI at pH 2, a large reduction peak using the polypyrrole was observed, which decreased by half as H_2O_2 was added (Figure S18). No current increase upon H_2O_2 addition occurred and even the opposite occurred, this can be regarded as a strong hint that PPy hinders a further reduction of H_2O_2 to water. Because of the large PPy reduction background current, no clear answer about the ORR from the K−L analysis was possible.

4. CONCLUSIONS

We explored PANI and PPy as potential electrocatalysts on carbon-based electrodes. On GC, PANI and PPy showed increased FEs at pH 7 from approximately 50−80% and 50−77%, respectively, while the absolute amount of H_2O_2 was not altered significantly. Hydrodynamic voltammetry revealed that the polymer coating hinders further reduction of produced H_2O_2. In acidic media, PANI acted as a *peroxide directing layer* preventing the direct 4-electron reduction of oxygen (O_2) to water (H_2O) (3). PPy on a high surface-area electrode such as CP at neutral pH significantly increased the amount of H_2O_2 produced from 85 $\mu mol_{H_2O_2}$ on blank CP more than three times up to 310 $\mu mol_{H_2O_2}$ after 6 h electrolysis. Simultaneously, the average FE compared to bare CP was improved from 25 to 96%.

From our studies, it can be concluded that electrochemically synthesized PANI is, in contrast to previous studies, an electrocatalyst but not showing a catalytic current increase. Nevertheless, the polymer coating on carbon electrodes considerably enhanced the long-term current efficiency by preventing undesired side or further reactions of H_2O_2 to H_2O. However, PPy prevented further reduction reactions and also showed electrocatalytic current increase upon O_2 addition. A possible explanation might be that PPy is oxidized by O_2; therefore, producing H_2O_2 and PPy by itself is getting re-reduced electrochemically.[33,40]

■ ASSOCIATED CONTENT

Supporting Information

The Supporting Information is available free of charge at https://pubs.acs.org/doi/10.1021/acsaem.0c01663.

> Optimization and description of the electrosynthetic procedures, H_2O_2 determination, FTIR and Raman spectra, further results from electrochemistry and SEM, and description of analysis of hydrodynamic voltammetry (PDF)

■ AUTHOR INFORMATION

Corresponding Author

Dominik Wielend − *Linz Institute for Organic Solar Cells (LIOS), Institute of Physical Chemistry, Johannes Kepler University Linz, Linz 4040, Austria*; orcid.org/0000-0003-1330-9915; Email: dominik.wielend@jku.at

Authors

Hannah Rabl − *Linz Institute for Organic Solar Cells (LIOS), Institute of Physical Chemistry, Johannes Kepler University Linz, Linz 4040, Austria*

Serpil Tekoglu − *Linz Institute for Organic Solar Cells (LIOS), Institute of Physical Chemistry, Johannes Kepler University Linz, Linz 4040, Austria*

Hathaichanok Seelajaroen − *Linz Institute for Organic Solar Cells (LIOS), Institute of Physical Chemistry, Johannes Kepler University Linz, Linz 4040, Austria*; orcid.org/0000-0002-1554-3644

Helmut Neugebauer − *Linz Institute for Organic Solar Cells (LIOS), Institute of Physical Chemistry, Johannes Kepler University Linz, Linz 4040, Austria*

Nikolas Heitzmann − *Linz Institute for Organic Solar Cells (LIOS), Institute of Physical Chemistry, Johannes Kepler University Linz, Linz 4040, Austria*

Dogukan Hazar Apaydin − *Linz Institute for Organic Solar Cells (LIOS), Institute of Physical Chemistry, Johannes Kepler University Linz, Linz 4040, Austria*

Markus Clark Scharber − *Linz Institute for Organic Solar Cells (LIOS), Institute of Physical Chemistry, Johannes Kepler University Linz, Linz 4040, Austria*; orcid.org/0000-0002-4918-4803

Niyazi Serdar Sariciftci − *Linz Institute for Organic Solar Cells (LIOS), Institute of Physical Chemistry, Johannes Kepler University Linz, Linz 4040, Austria*; orcid.org/0000-0003-4727-1193

Complete contact information is available at: https://pubs.acs.org/10.1021/acsaem.0c01663

Author Contributions

The manuscript was written through contributions of all authors. All authors have given approval to the final version of the manuscript.

Notes

The authors declare no competing financial interest.

■ ACKNOWLEDGMENTS

This work was financially supported by the European Regional Development Fund (EFRE) within the project "ENZYMBIOKAT" (GZ2018-98279-2). The authors gratefully acknowledge financial supports from the Austrian Science Foundation (FWF) within the Wittgenstein Prize for Prof. Sariciftci (Z222-N19).

■ TECHNICAL ABBREVIATIONS

ATR-FTIR, attenuated total reflection Fourier transformed infrared spectroscopy
CE, counter electrode
CNT, carbon nanotube
CP, carbon paper
CV, cyclic voltammetry
FE, faradaic efficiency
GC, glassy carbon
HER, hydrogen evolution reaction
I_D, disc current
I_R, ring current
j_P, peak current density
K−L, Koutecki−Levich analysis
LSV, linear sweep voltammetry
ORR, oxygen reduction reaction
RDE, rotating disc electrode
RE, reference electrode
RRDE, rotating ring disc electrode
SCE, saturated calomel electrode

SEM, scanning electron microscopy
SHE, standard hydrogen electrode
WE, working electrode

■ REFERENCES

(1) Lewis, N. S.; Nocera, D. G. Powering the Planet: Chemical Challenges in Solar Energy Utilization. *Proc. Natl. Acad. Sci. U.S.A.* **2006**, *103*, 15729−15735.
(2) Kalyanasundaram, K.; Graetzel, M. Artificial Photosynthesis : Biomimetic Approaches to Solar Energy Conversion and Storage. *Curr. Opin. Biotechnol.* **2010**, *21*, 298−310.
(3) Disselkamp, R. S. Can Aqueous Hydrogen Peroxide Be Used as a Stand-Alone Energy Source? *Int. J. Hydrogen Energy* **2010**, *35*, 1049−1053.
(4) Yamada, Y.; Fukunishi, Y.; Yamazaki, S.-i.; Fukuzumi, S. Hydrogen Peroxide as Sustainable Fuel: Electrocatalysts for Production with a Solar Cell and Decomposition with a Fuel Cell. *Chem. Commun.* **2010**, *46*, 7334−7336.
(5) Fukuzumi, S. Artificial Photosynthesis for Production of Hydrogen Peroxide and Its Fuel Cells. *Biochim. Biophys. Acta, Bioenerg.* **2016**, *1857*, 604−611.
(6) Goor, G.; Glenneberg, J.; Jacobi, S. Hydrogen Proxide. *Ullmann's Encyclopedia of Industrial Chemistry*, Wiley-VCH Verlag GmbH: Weinheim, 2012; Vol. *18*; pp 393−427.
(7) Uhl, A.; Bitzer, M.; Wolf, H.; Hermann, D.; Gutewort, S.; Völkl, M.; Nagl, I. Peroxy Compounds , Organic. *Ullmann's Encyclopedia of Industrial Chemistry*, Wiley-VCH Verlag GmbH: Weinheim, 2017; pp 1−45.
(8) Campos-Martin, J. M.; Blanco-Brieva, G.; Fierro, J. L. G. Hydrogen Peroxide Synthesis: An Outlook beyond the Anthraquinone Process. *Angew. Chem., Int. Ed.* **2006**, *45*, 6962−6984.
(9) Ragnar, M.; Henriksson, G.; Lindström, M. E.; Wimby, M.; Blechschmidt, J.; Heinemann, S. Pulp.. *Ullmann's Encyclopedia of Industrial Chemistry*, Wiley-VCH Verlag GmbH: Weinheim, 2014; Vol. *1*−*92*.
(10) Yamazaki, S.-i.; Siroma, Z.; Senoh, H.; Ioroi, T.; Fujiwara, N.; Yasuda, K. A Fuel Cell with Selective Electrocatalysts Using Hydrogen Peroxide as Both an Electron Acceptor and a Fuel. *J. Power Sources* **2008**, *178*, 20−25.
(11) An, L.; Zhao, T.; Yan, X.; Zhou, X.; Tan, P. The Dual Role of Hydrogen Peroxide in Fuel Cells. *Sci. Bull. formerly: Chi. Sci. Bull* **2015**, *60*, 55−64.
(12) Fukuzumi, S.; Yamada, Y. Hydrogen Peroxide Used as a Solar Fuel in One-Compartment Fuel Cells. *ChemElectroChem* **2016**, *3*, 1978−1989.
(13) Perry, S. C.; Pangotra, D.; Vieira, L.; Csepei, L.-I.; Sieber, V.; Wang, L.; Ponce de León, C.; Walsh, F. C. Electrochemical Synthesis of Hydrogen Peroxide from Water and Oxygen. *Nat. Rev.* **2019**, *3*, 442−458.
(14) Lu, Y.; Sehrish, A.; Manzoor, R.; Dong, K.; Jiang, Y. Recent Progress on Electrochemical Production of Hydrogen Peroxide. *Chem. Rep.* **2019**, *1*, 81−101.
(15) Meidinger, H. Ueber Voltametrische Messungen. *Justus Liebigs Ann. Chem.* **1853**, *88*, 57−81.
(16) Berl, E. A. New Cathodic Process for the Production of H2O2. *Trans. Electrochem. Soc.* **1939**, *2*, 359−369.
(17) Sun, Y.; Sinev, I.; Ju, W.; Bergmann, A.; Dresp, S.; Kühl, S.; Spöri, C.; Schmies, H.; Wang, H.; Bernsmeier, D.; Paul, B.; Schmack, R.; Kraehnert, R.; Roldan Cuenya, B.; Strasser, P. Efficient Electrochemical Hydrogen Peroxide Production from Molecular Oxygen on Nitrogen-Doped Mesoporous Carbon Catalysts. *ACS Catal.* **2018**, *8*, 2844−2856.
(18) Manchot, W. Ueber Sauerstoffactivirung. *Justus Liebigs Ann. Chem.* **1901**, *314*, 177−199.
(19) Jakešová, M.; Apaydin, D. H.; Sytnyk, M.; Oppelt, K.; Heiss, W.; Sariciftci, N. S.; Głowacki, E. D. Hydrogen-Bonded Organic Semiconductors as Stable Photoelectrocatalysts for Efficient Hydrogen Peroxide Photosynthesis. *Adv. Funct. Mater.* **2016**, *26*, 5248−5254.
(20) Warczak, M.; Gryszel, M.; Jakešová, M.; Đerek, V.; Głowacki, E. D. Organic Semiconductor Perylenetetracarboxylic Diimide (PTCDI) Electrodes for Electrocatalytic Reduction of Oxygen to Hydrogen Peroxide. *Chem. Commun.* **2018**, *54*, 1960−1963.
(21) Walsh, F. C.; Ponce de León, C. Progress in Electrochemical Flow Reactors for Laboratory and Pilot Scale Processing. *Electrochim. Acta* **2018**, *280*, 121−148.
(22) Wielend, D.; Vera-Hidalgo, M.; Seelajaroen, H.; Sariciftci, N. S.; Pérez, E. M.; Whang, D. R. Mechanically Interlocked Carbon Nanotubes as a Stable Electrocatalytic Platform for Oxygen Reduction. *ACS Appl. Mater. Interfaces* **2020**, *12*, 32615−32621.
(23) MacDiarmid, A. G.; Heeger, A. J. Organic Metals and Semiconductors: The Chemistry of Polyacetylene, (CH)x, and Its Derivatives. *Synth. Met.* **1980**, *1*, 101−118.
(24) *Handbook of Organic Conductive Molecules and Polymers*; Nalwa, H. S., Ed.; John Wiley & Sons, Inc.: Chichester, 1997; Vol. *1*−*4*.
(25) *Semiconducting Polymers: Chemistry, Physics and Engineering*; Hadziioannou, G., van Hutten, P. F., Eds.; Wiley-VCH Verlag GmbH: Weinheim, 1999.
(26) *Conjugated Polymers: Processing and Applications*, 3rd ed.; Skotheim, T. A., Reynolds, J., Eds.; CRC Press: Boca Raton, 2006.
(27) Shao, L.; Jeon, J.-W.; Lutkenhaus, J. L. Polyaniline/Vanadium Pentoxide Layer-by-Layer Electrodes for Energy Storage. *Chem. Mater.* **2014**, *24*, 181−189.
(28) Wang, H.; Lin, J.; Shen, Z. X. Polyaniline (PANi) Based Electrode Materials for Energy Storage and Conversion. *J. Sci. Adv. Mater. Devices* **2016**, *1*, 225−255.
(29) Hursán, D.; Kormányos, A.; Rajeshwar, K.; Janáky, C. Polyaniline Films Photoelectrochemically Reduce CO2 to Alcohols. *Chem. Commun.* **2016**, *52*, 8858−8861.
(30) Shi, Y.; Yu, G. Designing Hierarchically Nanostructured Conductive Polymer Gels for Electrochemical Energy Storage and Conversion. *Chem. Mater.* **2016**, *28*, 2466−2477.
(31) Werner, D.; Griesser, C.; Stock, D.; Griesser, U. J.; Kunze-Liebhäuser, J.; Portenkirchner, E. Substantially Improved Na-Ion Storage Capability by Nanostructured Organic−Inorganic Polyaniline-TiO2 Composite Electrodes. *ACS Appl. Energy Mater.* **2020**, *3*, 3477−3487.
(32) Rochliadi, A.; Akbar, S. A.; Suendo, V. Polyaniline/Zn as Secondary Battery for Electric Vehicle Base on Energy Return Factor. *Joint International Conference on Electric Vehicular Technology and Industrial, Mechanical, Electrical and Chemical Engineering (ICEVT IMECE)*, 2015; pp 353−358.
(33) Wu, A.; Venancio, E. C.; MacDiarmid, A. G. Polyaniline and Polypyrrole Oxygen Reversible Electrodes. *Synth. Met.* **2007**, *157*, 303−310.
(34) Li, W.; Gao, F.; Wang, X.; Zhang, N.; Ma, M. Strong and Robust Polyaniline-Based Supramolecular Hydrogels for Flexible Supercapacitors. *Angew. Chem., Int. Ed.* **2016**, *55*, 9196−9201.
(35) Marmisollé, W. A.; Gregurec, D.; Moya, S.; Azzaroni, O. Polyanilines with Pendant Amino Groups as Electrochemically Active Copolymers at Neutral PH. *ChemElectroChem* **2015**, *2*, 2011−2019.
(36) Tekoglu, S.; Wielend, D.; Scharber, M. C.; Sariciftci, N. S.; Yumusak, C. Conducting Polymer-Based Biocomposites Using Deoxyribonucleic Acid (DNA) as Counterion. *Adv. Mater. Technol.* **2019**, *5*, 1900699.
(37) Mengoli, G.; Musiani, M. M.; Zotti, G.; Valcher, S. Potentiometric Investigation of the Kinetics of the Polyaniline-Oxygen Reaction. *J. Electroanal. Chem.* **1986**, *202*, 217−230.
(38) Doubova, L.; Mengoli, G.; Musiani, M. M.; Valcher, S. Polyaniline as a Cathode for O2 Reduction-Kinetics of the Reaction with H2O2 and Use of the Polymer in a Model H2O2 Fuel Cell. *Electrochim. Acta* **1989**, *34*, 337−343.
(39) Cui, C. Q.; Lee, J. Y. Effect of Polyaniline on Oxygen Reduction in Buffered Neutral Solution. *J. Electroanal. Chem.* **1994**, *367*, 205−212.

https://dx.doi.org/10.1021/acsaem.0c01663
ACS Appl. Energy Mater. 2020, 3, 10611−10618

(40) Khomenko, V. G.; Barsukov, V. Z.; Katashinskii, A. S. The Catalytic Activity of Conducting Polymers toward Oxygen Reduction. *Electrochim. Acta* **2005**, *50*, 1675−1683.
(41) Miglbauer, E.; Wójcik, P. J.; Głowacki, E. D. Single-Compartment Hydrogen Peroxide Fuel Cells with Poly(3,4-Ethylenedioxythiophene) Cathodes. *Chem. Commun.* **2018**, *54*, 11873−11876.
(42) Mitraka, E.; Gryszel, M.; Vagin, M.; Jafari, M. J.; Singh, A.; Warczak, M.; Mitrakas, M.; Berggren, M.; Ederth, T.; Zozoulenko, I.; Crispin, X.; Głowacki, E. D. Electrocatalytic Production of Hydrogen Peroxide with Poly(3,4-Ethylenedioxythiophene) Electrodes. *Adv. Sustainable Syst.* **2019**, *3*, 1800110.
(43) Ramírez-Pérez, A. C.; Quílez-Bermejo, J.; Sieben, J. M.; Morallón, E.; Cazorla-Amorós, D. Effect of Nitrogen-Functional Groups on the ORR Activity of Activated Carbon Fiber-Polypyrrole-Based Electrodes. *Electrocatalysis* **2018**, *9*, 697−705.
(44) Hassan, M.; Qiu, W.; Song, X.; Mao, Q.; Ren, S.; Hao, C. Supercapacitive and ORR Performances of Nitrogen-Doped Hollow Carbon Spheres Pyrolyzed from Polystyrene@polypyrrole-Polyaniline. *J. Alloys Compd.* **2020**, *818*, 152890.
(45) Quílez-Bermejo, J.; González-Gaitán, C.; Morallón, E.; Cazorla-Amorós, D. Effect of Carbonization Conditions of Polyaniline on Its Catalytic Activity towards ORR. Some Insights about the Nature of the Active Sites. *Carbon* **2017**, *119*, 62−71.
(46) He, Y.; Han, X.; Du, Y.; Zhang, B.; Xu, P. Heteroatom-Doped Carbon Nanostructures Derived from Conjugated Polymers for Energy Applications. *Polymers* **2016**, *8*, 366.
(47) Sapurina, I.; Stejskal, J. Ternary Composites of Multi-Wall Carbon Nanotubes, Polyaniline, and Noble-Metal Nanoparticles for Potential Applications in Electrocatalysis. *Chem. Pap.* **2009**, *63*, 579−585.
(48) Drelinkiewicz, A.; Zięba, A.; Sobczak, J. W.; Bonarowska, M.; Karpiński, Z.; Waksmundzka-Góra, A.; Stejskal, J. Polyaniline Stabilized Highly Dispersed Pt Nanoparticles: Preparation, Characterization and Catalytic Properties. *React. Funct. Polym.* **2009**, *69*, 630−642.
(49) Wu, G.; More, K. L.; Johnston, C. M.; Zelenay, P. High-Performance Electrocatalysts for Oxygen Reduction Derived from Polyaniline, Iron, and Cobalt. *Science* **2011**, *332*, 443−447.
(50) Rafti, M.; Marmisollé, W. A.; Azzaroni, O. Metal-Organic Frameworks Help Conducting Polymers Optimize the Efficiency of the Oxygen Reduction Reaction in Neutral Solutions. *Adv. Mater. Interfaces* **2016**, *3*, 1600047.
(51) Fenoy, G. E.; Scotto, J.; Azcárate, J.; Rafti, M.; Marmisollé, W. A.; Azzaroni, O. Powering Up the Oxygen Reduction Reaction through the Integration of O2-Adsorbing Metal−Organic Frameworks on Nanocomposite Electrodes. *ACS Appl. Energy Mater.* **2018**, *1*, 5428−5436.
(52) Mártire, A. P.; Segovia, G. M.; Azzaroni, O.; Rafti, M.; Marmisollé, W. Layer-by-Layer Integration of Conudcting Polymers and Metal Organic Frameworks onto Electrode Surfaces : Enhancement of the Oxygen Reduction Reaction through Electrocatalytic Nanoarchtiectonics. *Mol. Syst. Des. Eng.* **2019**, *4*, 893−900.
(53) Abe, T.; Kaneko, M. Reduction Catalysis by Metal Complexes Confined in a Polymer Matrix. *Prog. Polym. Sci.* **2003**, *28*, 1441−1488.
(54) Ramohlola, K. E.; Masikini, M.; Mdludli, S. B.; Monama, G. R.; Hato, M. J.; Molapo, K. M.; Iwuoha, E. I.; Modibane, K. D. Electrocatalytic Hydrogen Production Properties of Polyaniline Doped with Metal- Organic Frameworks. In *Carbon-related Materials in Recognition of Nobel Lectures by Prof. Akira Suzuki in ICCE*; Kaneko, S., Mele, P., Endo, T., Tsuchiya, T., Tanaka, K., Yoshimura, M., Hui, D., Eds.; Springer: Cham, 2017; pp 373−389.
(55) Coskun, H.; Aljabour, A.; Schöfberger, W.; Hinterreiter, A.; Stifter, D.; Sariciftci, N. S.; Stadler, P. Cofunction of Protons as Dopant and Reactant Activate the Electrocatalytic Hydrogen Evolution in Emeraldine- Polyguanine. *Adv. Mater. Interfaces* **2019**, *7*, 1901364.
(56) Nunziante, P.; Pistoia, G. Factors Affecting the Growth of Thick Polyaniline Films by the Cyclic Voltammetry Technique. *Electrochim. Acta* **1989**, *34*, 223−228.
(57) Sariciftci, N. S.; Bartonek, M.; Kuzmany, H.; Neugebauer, H.; Neckel, A. Analysis of Various Doping Mechainsms in Polyaniline by Optical , FTIR and Raman Spectroscopy. *Synth. Met.* **1989**, *29*, 193−202.
(58) Andriukonis, E.; Ramanaviciene, A.; Ramanavicius, A. Synthesis of Polypyrrole Induced by [Fe(CN)6]3- and Redox Cycling of [Fe(CN)6]4-/[Fe(CN)6]3-. *Polymers* **2018**, *10*, 749.
(59) Su, G.; Wei, Y.; Guo, M. Direct Colorimetric Detection of Hydrogen Peroxide Using 4-Nitrophenyl Boronic Acid or Its Pinacol Ester. *Am. J. Anal. Chem.* **2011**, *02*, 879−884.
(60) Apaydin, D. H.; Seelajaroen, H.; Pengsakul, O.; Thamyongkit, P.; Sariciftci, N. S.; Kunze-Liebhäuser, J.; Portenkirchner, E. Photoelectrocatalytic Synthesis of Hydrogen Peroxide by Molecular Copper-Porphyrin Supported on Titanium Dioxide Nanotubes. *ChemCatChem* **2018**, *10*, 1793−1797.
(61) Song, E.; Choi, J.-W. Conducting Polyaniline Nanowire and Its Applications in Chemiresistive Sensing. *Nanomaterials* **2013**, *3*, 498−523.
(62) Taylor, R. J.; Humffray, A. A. Electrochemical Studies on Glassy Carbon Electrodes II*. Oxygen Reduction in Solutions of High PH (PH>10). *J. Electroanal. Chem.* **1975**, *64*, 63−84.
(63) Taylor, R. J.; Humffray, A. A. Electrochemical Studies on Glassy Carbon Electrodes III. Oxygen Reduction in Solutions of Low PH (PH<10). *J. Electroanal. Chem.* **1975**, *64*, 85−94.